

# Radial Velocity Studies of Close Binary Stars. IX<sup>1</sup>

Wojtek Pych<sup>2</sup>, Slavek M. Rucinski, Heide DeBond, J. R. Thomson, Christopher C. Capobianco,  
R. Melvin Blake

*David Dunlap Observatory, University of Toronto  
P.O. Box 360, Richmond Hill, Ontario, Canada L4C 4Y6*

(pych,rucinski,debond,jthomson,capobianco,blake)@astro.utoronto.ca

and

Waldemar Ogłóza

*Mt. Suhora Observatory of the Pedagogical University  
ul. Podchorążych 2, 30-084 Cracow, Poland*

ogloza@ap.krakow.pl

and

Greg Stachowski

*Copernicus Astronomical Center, Bartycka 18, 00-716 Warszawa, Poland*

gss@camk.edu.pl

and

Piotr Rogoziecki, Piotr Ligeza

*Adam Mickiewicz University Observatory, Słoneczna 36, 60-286 Poznań, Poland*

progoz@moon.astro.amu.edu.pl, piotrl@amu.edu.pl

and

Kosmas Gazeas

*Department of Astrophysics, Astronomy and Mechanics  
National & Kapodistrian University of Athens, GR 157 84 Zographou, Athens, Greece*

kgaze@skiathos.physics.auth.gr

## ABSTRACT

---

<sup>2</sup>On leave from: Copernicus Astronomical Center, Bartycka 18, 00-716 Warszawa, Poland

Radial-velocity measurements and sine-curve fits to the orbital velocity variations are presented for the eighth set of ten close binary systems: AB And, V402 Aur, V445 Cep, V2082 Cyg, BX Dra, V918 Her, V502 Oph, V1363 Ori, KP Peg, V335 Peg. Half of the systems (V445 Cep, V2082 Cyg, V918 Her, V1363 Ori, V335 Peg) were discovered photometrically by the *Hipparcos* mission and all systems are double-lined (SB2) contact binaries. The broadening function method permitted improvement of the orbital elements for AB And and V502 Oph. The other systems have been observed for radial velocity variations for the first time; in this group are five bright ( $V < 7.5$ ) binaries: V445 Cep, V2082 Cyg, V918 Her, KP Peg and V335 Peg. Several of the studied systems are prime candidates for combined light and radial-velocity synthesis solutions.

*Subject headings:* stars: close binaries - stars: eclipsing binaries – stars: variable stars

## 1. INTRODUCTION

This paper is a continuation in a series of papers of radial-velocity studies of close binary stars (Lu & Rucinski 1999; Rucinski & Lu 1999; Rucinski, Lu, & Mochnacki 2000; Lu, Rucinski, & Ogloza 2001; Rucinski et al. 2001, 2002, 2003) and presents data for the eighth group of ten close binary stars observed at the David Dunlap Observatory. Selection of the targets is quasi-random: At a given time, we observe a few dozen close binary systems with periods shorter than one day, brighter than 11 magnitude and with declinations  $> -15^\circ$ . We publish the results in groups of ten systems as soon as reasonable orbital elements are obtained from measurements evenly distributed in orbital phases. For technical details and conventions, and for preliminary estimates of errors and uncertainties, see the interim summary paper Rucinski (2002a, hereafter Paper VII). With this paper, we decided to introduce some minor changes into the reduction process: We used the pair of IRAF routines *noao.imred.spec.fitcoords* and *noao.imred.spec.transform* to rectify images of the spectra and improve wavelength calibrations; the procedure of cosmic ray removal was done using a separate, standalone program (Pych 2003).

We estimate spectral types of the program stars using our classification spectra. These are compared with the mean ( $B - V$ ) color indexes taken from the *Tycho-2* catalog (Høg et al. 2000) and the photometric estimates of the spectral types using the relations published by Bessell (1979).

The observations reported in this paper have been collected mostly during the year 2002; exceptions are: BX Dra and V335 Peg, for which some observations were collected in 2001, and V918 Her, for which some observations were in May 2003. The ranges of dates for individual systems can be found in Table 1.

---

<sup>1</sup>Based on the data obtained at the David Dunlap Observatory, University of Toronto.

Table 2. Spectroscopic orbital elements

Name	Type Sp. type	Other names	$V_0$	$K_1$ $K_2$	$\epsilon_1$ $\epsilon_2$	$T_0 - 2,400,000$ (O–C)(d) [E]	P (days) $(M_1 + M_2) \sin^3 i$	$q$
AB And	EW/W	SAO 73069	–27.53(0.67)	130.32(1.17)	5.13	52,503.0443(4)	0.3318919	0.560(7)
	G8V	HIP 114508		232.88(0.83)	8.20	–0.0105 [–2957]	1.648(20)	
V402 Aur	EW/W	HD 282719	+40.82(0.93)	41.94(0.83)	4.33	52,448.9698(16)	0.603491	0.201(6)
	F2V	HIP 23433		208.98(2.17)	13.46	+0.0008 [371]	0.988(27)	
V445 Cep	EW/A	HD 210431	+40.69(0.95)	20.33(0.85)	4.57	52,470.5847(21)	0.448776	0.167(10)
	A2V	HIP 109191		122.08(2.04)	11.55	+0.0072 [8847]	0.134(6)	
V2082 Cyg	EW/A:	HD 183752	–34.12(0.58)	33.16(0.51)	2.85	52,466.1122(17)	0.714084	0.238(5)
	F2V	HIP 95833		139.38(0.99)	6.75	–0.0249 [5554]	0.380(7)	
BX Dra	EW/A	HIP 78891	–26.11(3.43)	80.01(2.46)	8.87	52,248.2984(34)	0.579027	0.289(16)
	F0IV-V			276.39(6.37)	23.90	+0.0006 [6473]	2.72(16)	
V918 Her	EW/W	HD 151701	–25.72(0.74)	53.93(0.49)	3.45	52,555.8419(14)	0.57481	0.271(5)
	A7V	HIP 82253		199.37(1.72)	10.43	+0.0253 [7055]	0.968(21)	
V502 Oph	EW/W	HD 150484	–42.56(0.85)	82.71(1.03)	6.38	52,452.7492(7)	0.45339	0.335(9)
	G0V	HIP 81703		246.70(1.00)	6.89	–0.0500 [8718]	1.679(22)	
V1363 Ori	EW/A	HD 289949	+37.89(2.02)	44.88(2.46)	16.32	52,592.4999(20)	0.431921	0.205(15)
	F: <sup>a</sup>	HIP 23809		219.30(4.18)	21.62	+0.0196 [9475]	0.825(45)	
KP Peg	EW/A	HD 204215	+5.52(1.03)	72.84(1.05)	6.20	52,504.9303(21)	0.727203	0.322(10)
	A2V	HIP 105882		226.43(4.10)	18.18	+0.0214 [5507]	2.020(86)	
V335 Peg	EW/A:	HD 216417	–15.41(0.43)	44.61(0.27)	2.47	52,330.1642(15)	0.810720	0.262(4)
	F5V	HIP 112960		170.56(1.77)	12.54	–0.1590 [4724]	0.837(21)	

<sup>a</sup>V1363 Ori: Early to mid F-type

Note. — The spectral types given in column two are all new and relate to the combined spectral type of all components in a system. The convention of naming the binary components in this table is that the more massive star is marked by the subscript “1”, so that the mass ratio is defined to be always  $q \leq 1$ . Figures 1 – 3 should help identify which component is eclipsed at the primary minimum. The standard errors of the circular solutions in the table are expressed in units of last decimal places quoted; they are given in parantheses after each value. The center-of-mass velocities ( $V_0$ ), the velocity amplitudes ( $K_i$ ) and the standard unit-weight errors of the solutions ( $\epsilon$ ) are all expressed in  $\text{km s}^{-1}$ . The spectroscopically determined moments of primary minima are given by  $T_0$ ; the corresponding ( $O - C$ ) deviations (in days) have been calculated from the most recent available ephemerides, as given in the text, using the assumed periods and the number of epochs given by [E]. The values of  $(M_1 + M_2) \sin^3 i$  are in the solar mass units.

All systems discussed in this paper, except AB And and V502 Oph, have been observed for radial-velocity variations for the first time. We have derived the radial velocities in the same way as described in previous papers. See Paper VII for a discussion of the broadening-function approach used in the derivation of the radial-velocity orbit parameters: the amplitudes,  $K_i$ , the center-of-mass velocity,  $V_0$ , and the time-of-primary-eclipse epoch,  $T_0$ .

This paper is structured in a way similar to that of previous papers, in that most of the data for the observed binaries are in two tables consisting of the radial-velocity measurements (Table 1) and their sine-curve solutions (Table 2). The data in Table 2 are organized in the same manner as in previous papers. In addition to the parameters of spectroscopic orbits, the table provides information about the relation between the spectroscopically observed epoch of the primary-eclipse  $T_0$  and the recent photometric determinations in the form of the  $O-C$  deviations for the number of elapsed periods  $E$ . It also contains our new spectral classifications of the program objects. Section 2 of the paper contains brief summaries of previous studies for individual systems and comments on the new data. Figures 1 – 3 show the radial velocity data and solutions. Figure 4 shows the BF’s for all systems; the functions have been selected from among the best defined ones around the orbital phase of 0.25 using the photometric system of phases counted from the deeper eclipse.

## 2. RESULTS FOR INDIVIDUAL SYSTEMS

### 2.1. AB And

Photometric variability of AB And was discovered by Guthnik & Prager (1927). Oosterhoff (1930) gave a photometric ephemeris. Twenty years later, Oosterhoff (1950) reported discovery of the period variation. Since that time, AB And became a target of numerous photometric investigations. On the basis of the photoelectric observations, Landolt (1969) determined the spectral type of K2V. He also noted asymmetries in the light curve. The asymmetries have been explained in Bell, Hilditch, & King (1984) and Djurasevic, Rovithis-Livaniou, & Rovithis (2000) by a model with photospheric spots. Demircan et al. (1994) suggested that observed period variability may be a result of the orbital motion in a wide triple system. The third body should be a white dwarf in such a case. Strömngren photometry presented by Rucinski & Kaluzny (1981) suggested the spectral type of AB And to be G5.

The first spectroscopic observations of this object were published by Struve et al. (1950). AB And was then classified as a W UMa star with spectral type G5. The radial velocities of the components were measured in this investigation in only 7 spectra, therefore this result was rather preliminary. The results were:  $V_0 = -45 \text{ km s}^{-1}$ ,  $K_1 = 165 \text{ km s}^{-1}$  and  $K_2 = 265 \text{ km s}^{-1}$ . An extensive discussion on the system with the combined light and radial-velocity solution was presented by Hrivnak (1988) who classified the spectral type of AB And to be G5V. Radial velocity curves obtained by Hrivnak (1988) were modified to include proximity effects. The measured radial velocities gave following orbital parameters:  $V_0 = -24.6 \pm 0.9 \text{ km s}^{-1}$   $K_1 = 115.7 \pm 0.7 \text{ km s}^{-1}$  and

$$K_2 = 235.7 \pm 1.5 \text{ km s}^{-1}.$$

For the preliminary moment of eclipse  $T_0$ , as referred to in Table 2, we used the moment of Pribulla et al. (2002). Similar to the previous researchers, we find the system to be a W-type contact binary. Our spectral type, G8V, is slightly later than most of the previous determinations. AB And has relatively red color index  $(B - V) = 0.925$ , which corresponds to the spectral type K2. Spots in the photospheres of the system components may be a possible explanation of the spectral type discrepancy. The broadening functions of both system components are well defined and radial velocities are measured precisely. We note a difference in the center-of-mass velocity of the system between our estimate:  $V_0 = -27.5 \pm 0.7 \text{ km s}^{-1}$  and the result presented by Hrivnak (1988). Also, the amplitude of radial velocity of the less massive component obtained by Hrivnak (1988) was smaller than our result,  $K_1 = 130.3 \text{ km s}^{-1}$ , possibly because Hrivnak (1988) used the cross-correlation method which – in our experience – frequently under-estimates the velocity amplitudes.

The Hipparcos parallax,  $8.34 \pm 1.48 \text{ mas}$  (milli-arcsec), gives the distance of  $120 \pm 20 \text{ pc}$ . The observed proper motion is moderately large (Høg et al. 2000), resulting, for the assumed distance, in tangential velocities of  $V_{RA} = 109 \text{ km s}^{-1}$  and  $V_{dec} = -53 \text{ km s}^{-1}$  and the combined spatial velocity of  $V = 74 \text{ km s}^{-1}$ . Because the observed variability of the period and of  $V_0$  can be interpreted as an influence of a companion, the parallax may be incorrect; the large error is consistent with that. The direct, parallax-based estimate of  $M_V = 4.1 \pm 0.4$  only marginally agrees with the one from the absolute-magnitude calibration (Rucinski & Duerbeck 1997),  $M_V(cal) = 5.0$ ; however,  $V_{max} = 9.5$  is also poorly defined, partly because of the spots and partly because of the small number of calibrated light curves even for this popular system.

The masses of the components are very well defined,  $M_1 \sin^3 i = 1.06 M_\odot$  and  $M_2 \sin^3 i = 0.59 M_\odot$ , and are surprisingly large for components of a G8/K2 contact system. We have seen a very similar situation in AH Vir (Lu & Rucinski 1993), which is also a system consisting of massive but unusually cool components. It is very likely that the strong magnetic activity of AB And and AH Vir may have something to do with this anomaly.

## 2.2. V402 Aur

V402 Aur was discovered as a variable by Oja (1991) during an UBV photometric survey of astrometric standard stars. The light-curve and ephemeris were published 3 years later (Oja 1994). The spectral type derived from Henry Draper Extension Charts is F0 (Nesterow et al. 1995). Spectral type in the SIMBAD database is F2. The spectral type corresponding to  $(B - V) = 0.40$  derived from the *Tycho-2* catalog (Høg et al. 2000) is F3-4. Our new spectral type is F2V.

The mass ratio is small,  $q = 0.20$ . Similar depths of the eclipses and the well defined broadening functions strongly suggests that V402 Aur is a contact binary of the W-type (with the assumed moment of the primary eclipse, as referred to in Table 2, of Pribulla et al. (2002)). The small sum

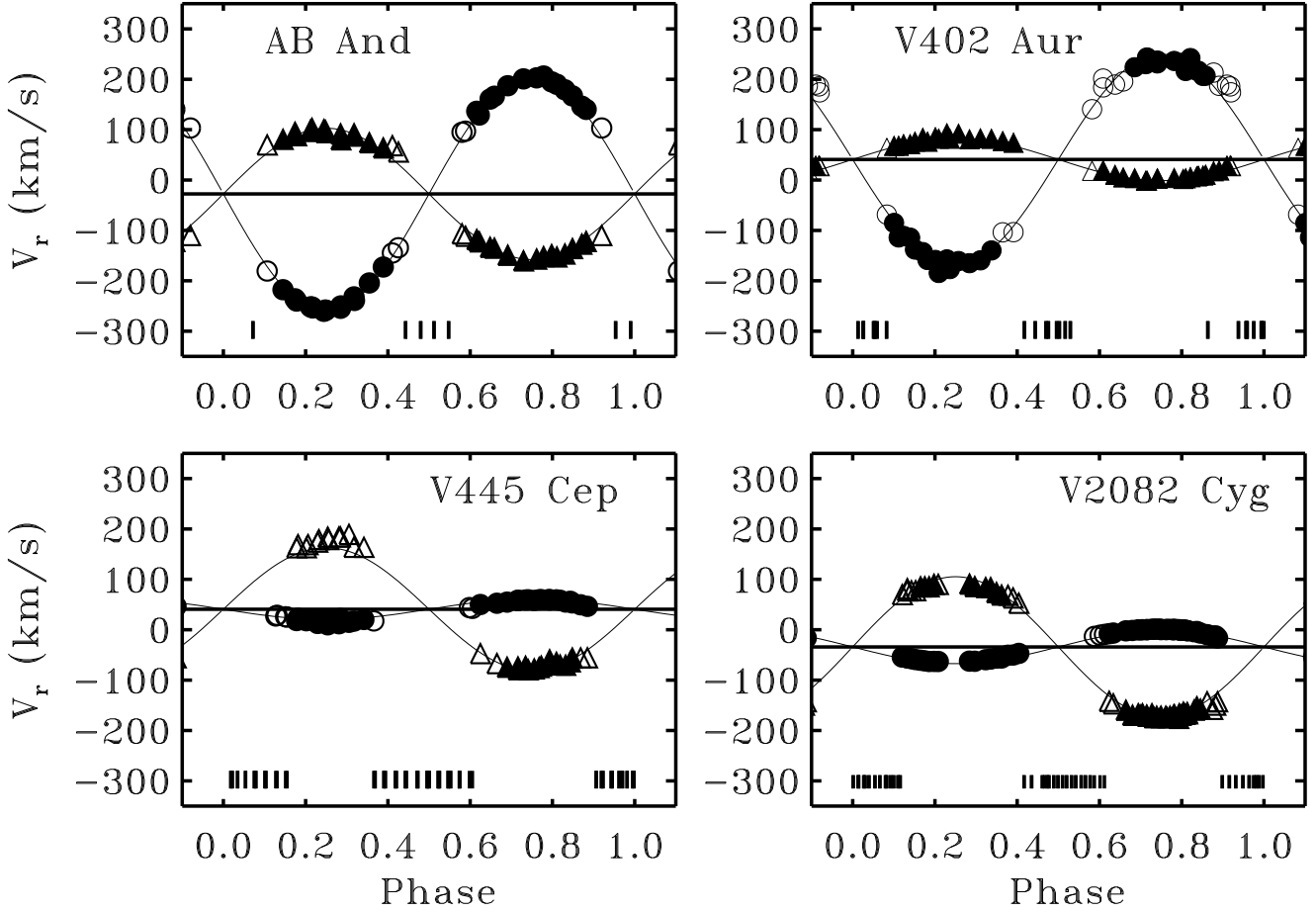


Fig. 1.— Radial velocities of the systems AB And, V402 Aur, V445 Cep and V2082 Cyg are plotted in individual panels versus the orbital phases. All four systems are contact binaries. V445 Cep and V2082 Cyg are A-type contact systems, while AB And and V402 Aur are W-type contact systems. The lines give the respective circular-orbit (sine-curve) fits to the radial velocities. The circles and triangles in this and the next two figures correspond to components with velocities  $V_1$  and  $V_2$ , as listed in Table 1, respectively. The component eclipsed at the minimum corresponding to  $T_0$  (as given in Table 2) is the one which shows negative velocities for the phase interval 0.0 – 0.5. The open symbols indicate observations contributing half-weight data in the solutions. Short marks in the lower parts of the panels show phases of available observations which were not used in the solutions because of the blending of lines. All panels have the same vertical range,  $-350$  to  $+350$  km s $^{-1}$ .

of the masses for an early-F system,  $(M_1 + M_2) \sin^3 i = 0.99 \pm 0.03 M_\odot$ , is consistent with the small photometric amplitude of 0.17 mag., both being due to the low inclination of the orbit.

### 2.3. V445 Cep

Variability of V445 Cep was discovered by *Hipparcos*. The full amplitude of the *Hipparcos* light-curve is only 0.03 mag. The star has abnormally blue color index for its period (Rucinski 2002b), which raised a suspicion that pulsations are the source of the observed photometric variability. Our radial velocity observations confirm the binary nature of the system, but with the period equal to twice the *Hipparcos* period. We adjusted the preliminary *Hipparcos*  $T_0$  by one quarter forward of the light maximum to  $T_0 = 2,448,500.1146$ .

The mass ratio of V445 Cep,  $q = 0.17 \pm 0.01$ , is small. We also find a very small value of  $(M_1 + M_2) \sin^3 i = 0.134 \pm 0.006 M_\odot$ . This result, together with small photometric amplitude, suggest a small inclination angle of the orbit. The system seems to be a contact binary, but small amplitudes of radial velocities and photometric variability make it difficult to derive the orbital parameters.

The results of low-resolution spectroscopic observations were presented by Grenier et al. (1999). The star was classified as A2V. The radial velocity of the whole system  $V_r = 38.6 \pm 9.6 \text{ km s}^{-1}$  is in a good agreement with our  $V_0 = 40.69 \pm 0.95 \text{ km s}^{-1}$ .

The color index  $(B - V) = 0.123$  was found in the *Tycho-2* catalog (Høg et al. 2000). This corresponds to a spectral type A4. Our spectral type is A2V. The system is bright,  $V_{max} = 6.82$ , which together with the *Hipparcos* parallax gives,  $M_V = 1.58 \pm 0.13$ . Thus, this is one of the best determined luminosities for an A spectral-type contact binary.

### 2.4. V2082 Cyg

This star was listed as a variable candidate by Hoffleit (1979). It's variability was confirmed by *Hipparcos*. The light-curve from *Hipparcos* has a small amplitude of only 0.05 mag and similar depths of the eclipses. We used the *Hipparcos* data for the preliminary  $T_0$ .

The spectral type of V2082 Cyg in the SIMBAD database is F0, while our spectral type is F2V.  $(B - V) = 0.313$  from *Tycho-2* catalog (Høg et al. 2000) corresponds to the spectral type F1. V2082 Cyg is most probably an A-type contact binary, although the secondary component is faint (the relative luminosity from the broadening function,  $L_2 = 0.10 \pm 0.02$ ), so that we cannot exclude a semi-detached configuration. The system must be viewed at a very low inclination angle which would explain the small photometric and radial velocity amplitudes, leading too poorly resolved broadening functions, with the partly merged signatures of both components (see Fig. 4).

The absolute magnitude based on the *Hipparcos* parallax and the adopted  $V_{max} = 6.64$  is  $M_V = 1.85 \pm 0.12$ . It agrees well with the RD97 calibration,  $M_V(cal) = 1.71$ . The proper motion, especially in declination, is large (Høg et al. 2000), resulting, for the assumed distance, in the combined spatial velocity of  $V = 54 \text{ km s}^{-1}$ .

The radial velocity of the system was previously measured at low resolution by Shajn (1951) on three occasions. The author noticed that the radial velocity of this star is variable.

## 2.5. BX Dra

BV 228 (BX Dra) was discovered to be a variable star by Strohmeier (1958). Strohmeier et al. (1965) classified the star as an RR Lyrae type variable. Some doubt to this classification and hints about the binary nature of the star based both on spectroscopy and photometry were presented by Smith (1990). The author, in a photometric survey of variable stars, found a new period and changed the classification to an elliptical variable. Independently, Agerer & Dahm (1995) presented a light-curve and classified BX Dra as an  $\beta$  Lyr type variable. Nevertheless Solano et al. (1997) still regarded it as a RR Lyr variable, although they have found some other stars to be incorrectly classified as RR Lyr variables in the General Catalogue of Variable Stars (Kholopov et al. 1985-1988). SIMBAD still lists this star as a variable star of RR Lyr type. The spectral type of BX Dra in the SIMBAD database is A3.

We found that the variable is definitely a contact binary of the A-type. The color index  $(B - V) = 0.352$  from *Tycho-2* catalog (Høg et al. 2000) corresponds to the spectral type of F2. Our spectral type is F0IV-V. The star is one of the faintest in our sample ( $V_{max} = 10.5$ ) and the broadening functions are noisy and show undesirable baseline slopes (see Fig. 4). However, because the radial velocity amplitudes are relatively large, this object may deserve further photometric and spectroscopic investigations.

The radial velocity has been measured by Layden (1994) at low resolution,  $V_r = 75 \pm 30 \text{ km s}^{-1}$ . The radial velocity was also measured again by Solano et al. (1997), and the result  $V_r = -24 \pm 3 \text{ km s}^{-1}$ , is in agreement with our result  $V_r = -26.11 \pm 3.43 \text{ km s}^{-1}$  within the respective errors. The moment of the primary eclipse referred to in Table 2 was taken from the *Hipparcos* catalog.

## 2.6. V918 Her

Variability of this star was discovered by *Hipparcos*. The spectral type of this star in the SIMBAD database is A2. Grenier et al. (1999) classified its spectrum as A5V. Our spectral classification of V918 Her is A7V. The  $(B - V)$  index from the *Tycho-2* catalog (Høg et al. 2000) is 0.249 and corresponds to a spectral type A8/9V, which may indicate some reddening.

The radial velocity of the system measured by Grenier et al. (1999)  $V_r = -33.9 \pm 7.2 \text{ km s}^{-1}$



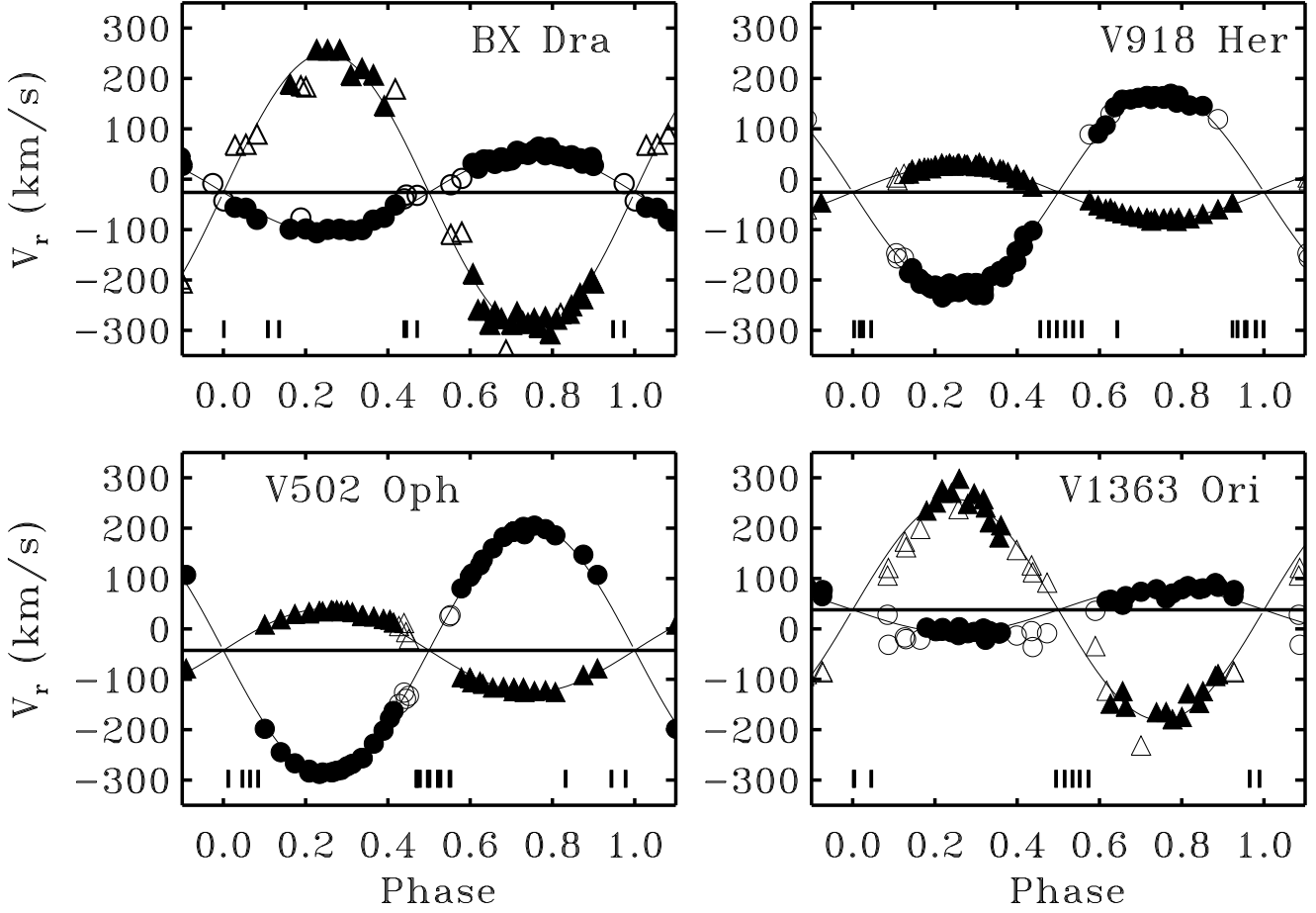


Fig. 2.— Same as for Figure 1, but with the radial velocity orbits for the systems BX Dra, V918 Her, V502 Oph and V1363 Ori. BX Dra and V1363 Ori are A-type contact systems, while V918 Her and V502 Oph are W-type contact systems.

is different from our result of  $V_r = -25.72 \pm 0.74 \text{ km s}^{-1}$ .

We find the object to be an A-type contact binary. Otherwise the system is rather inconspicuous, but is bright,  $V_{max} = 7.30$ , and thus was included in the magnitude-limited sample of Rucinski (2002b). We have adopted  $T_0$  from the *Hipparcos* catalog.

## 2.7. V502 Oph

V502 Oph was discovered to be an eclipsing binary by Hoffmeister (1935). The first ephemeris based on visual observations was published by Lause (1937). Over the years, the star has been the subject of numerous investigations. The light curve of the system is not stable and the orbital period was found to undergo a change in the years 1955–1966 (Binnendijk 1969). The period is successively decreasing, but the rate of the change observed in the years 1989 – 2003 has not been constant (Kreiner 2003). For Table 2, we adopted  $T_0$  from the *Hipparcos* catalog. We found however, that the orbital period from the *Hipparcos* catalog definitely does not fit our spectral data. We established that the period which fits our data best is 0.453390 days and this period was used for calculating the orbital elements in Table 2.

Observations of V502 Oph with the VLA revealed that it is a binary radio source (Hughes & McLean 1984). Since W UMa-type systems usually show low radio activity (Rucinski 1995), this may suggest the existence of an optically undetected companion to the eclipsing binary system (Hughes & McLean 1984). The presence of a late-type tertiary component was in fact noticed in the spectrum of V502 Oph by Hendry & Mochnacki (1998).

The pioneering investigation on the radial velocity orbit of this W UMa type variable was done by Gratton (as described in Struve & Gratton (1948)). The derived orbit elements based on these old observations,  $V_r = -37 \text{ km s}^{-1}$ ,  $K_1 = 95 \text{ km s}^{-1}$ ,  $K_2 = 235 \text{ km s}^{-1}$ , are surprisingly close the values presented in Table 2. Radial velocity measurements presented later by Struve & Zebergs (1959) generally supported earlier results; the  $-13 \text{ km s}^{-1}$  shift in the mass-center velocity was considered insignificant in view of the low accuracy of the measurements. The spectra of the components were classified as G1V for the primary and F9V for the secondary component, reflecting the fact that this is a W-type contact system with a slightly hotter secondary.

The spectral type in the SIMBAD database is "G2V+...". The spectral type of V502 Oph based on the *Tycho-2* color index (Høg et al. 2000),  $(B - V) = 0.615$ , is G1, which is close to G0V found by us.

## 2.8. V1363 Ori

The variability of V1363 Ori was discovered by *Hipparcos*. The spectral type derived from Henry Draper Extension Charts is F5 (Nesterow et al. 1995), while in the SIMBAD database it is

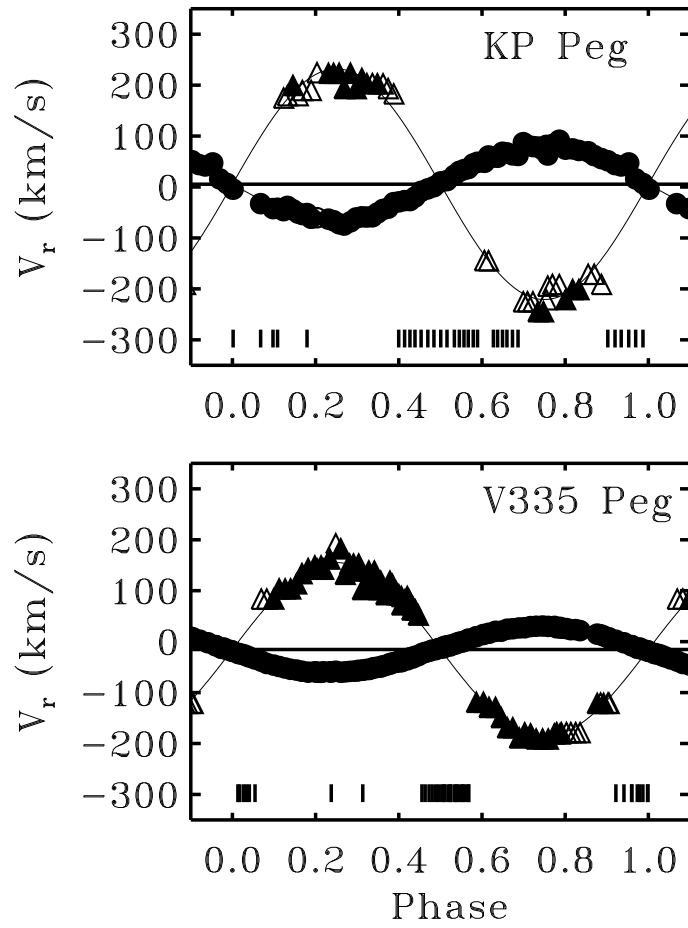


Fig. 3.— Same as for Figure 1, but with the radial velocity orbits for the systems KP Peg and V335 Peg. Both systems are A-type contact binaries.

F8. The  $(B - V) = 0.56$  color index derived from the *Tycho-2* catalog (Høg et al. 2000) corresponds to a spectral type of F9. For technical reasons, we were not able to obtain a good classification spectrum of the star; we can only confine it to the early to mid-F spectral type.

The light-curve of this variable presented by Gomez-Forrellad et al. (1999) shows the O’Connell effect. This source was used for the initial  $T_0$ .

V1363 Ori is an A-type contact binary at the faint end of our magnitude accessibility, so that the broadening functions are rather poor. The *Hipparcos* parallax is poorly determined,  $9.47 \pm 2.36$ , so that the binary may have a spectroscopically undetectable companion.

## 2.9. KP Peg

This star was listed as a suspected variable by Hopmann (1948). Walker (1987) confirmed that the component A of this visual binary system (separation 3.5 arcsec, magnitude difference 1.6) is a variable of Beta Lyrae type. He also gave its ephemeris and presented the light-curve (Walker 1988). Abt (1985), in one of his spectral classification papers of binaries from the Aitken (1932) catalog (ADS), classified it as an A2V star. We confirm this spectral type. It is also consistent with the  $(B - V) = 0.060$  color index from the *Tycho-2* catalog (Høg et al. 2000). Due to the early spectral type and the weak spectral lines in our standard spectral window, the broadening functions are rather poorly defined, with the component signatures partly merged in the broadening functions.

The *Hipparcos* parallax,  $4.37 \pm 1.67$  mas, is poorly determined, probably because of the presence of the third body in the system. With the corrected  $V_{max} = 7.07$  (Rucinski 2002b), the absolute magnitude of the binary is one of the brightest in our program,  $M_V = +0.3 \pm 0.8$ . The adopted  $T_0$  is from the *Hipparcos* catalog.

## 2.10. V335 Peg

Variability of V335 Peg was discovered by *Hipparcos*. The light-curve from *Hipparcos* has a small amplitude of 0.05 mag. It is most probably an A-type contact binary, although the broadening function of the secondary component is very weak (the relative luminosity determined from the broadening function is only  $L_2 = 0.05 \pm 0.01$ ) and is difficult to measure, contrary to that for the primary component whose velocity could be measured very precisely. At this point we cannot exclude a semi-detached configuration.

When we phased the observations, we noticed a small – about  $3.5 \text{ km s}^{-1}$ , systematic shift in radial velocities of the primary component between seasons 2001 and 2002. We have found that a correction to the period derived from *Hipparcos* light-curve may eliminate this discrepancy. The orbital solution presented in Table 2 has been obtained with the new period,  $P=0.81072$  days, but

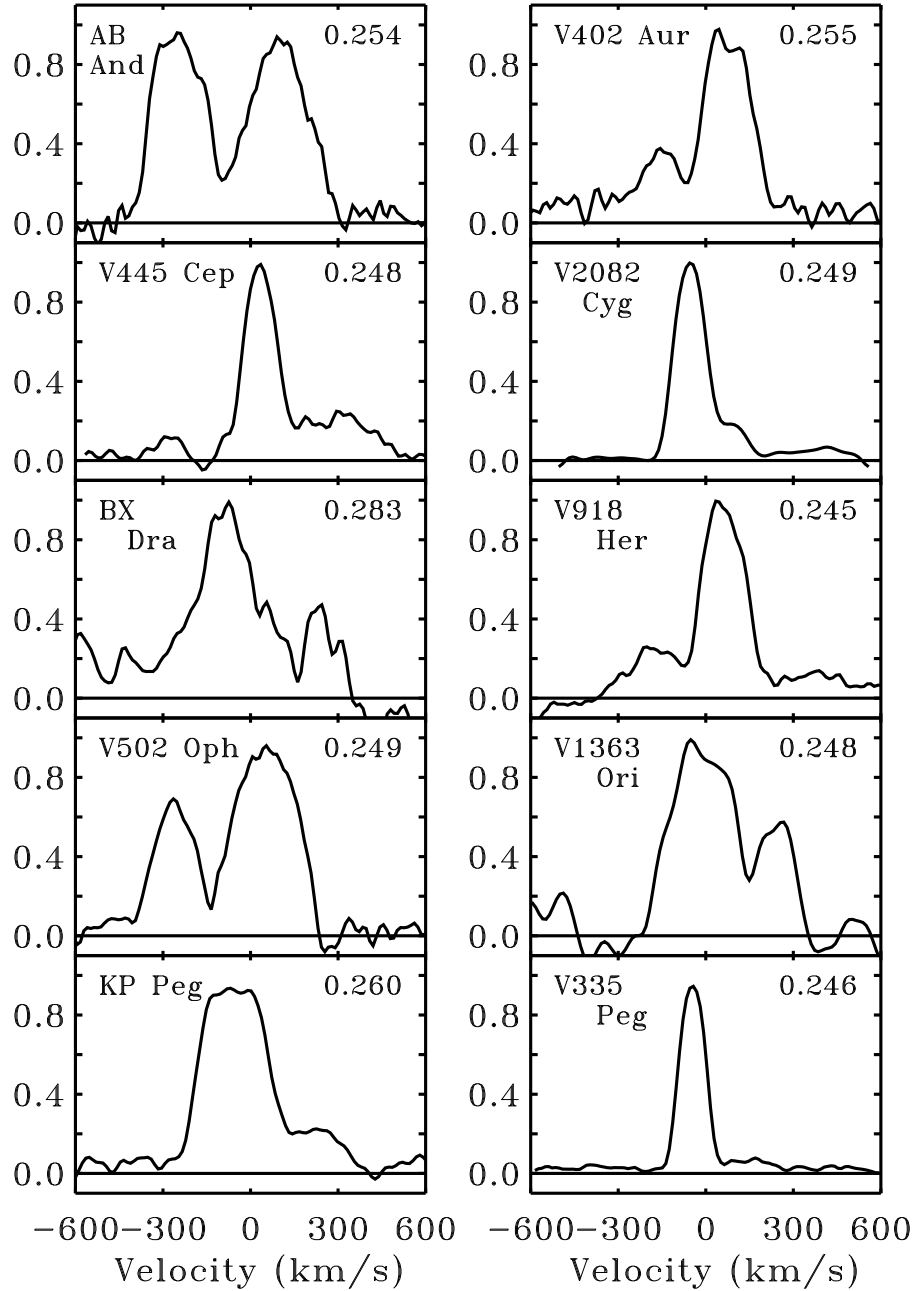


Fig. 4.— The broadening functions (BF's) for all binary systems of this group; all for orbital phases around 0.25, as in similar figures in the previous papers.

with the same  $T_0$ . We note that this period implies a large  $T_0$  shift of  $O - C = -0.159$  days. The orbital parameters obtained for the *Hipparcos* period:  $P=0.810746$  days,  $V_0 = -15.85 \pm 0.47$  km s<sup>-1</sup>,  $K_1 = 45.52 \pm 0.33$  km s<sup>-1</sup>,  $K_2 = 169.58 \pm 1.77$  km s<sup>-1</sup>, result in a smaller  $O - C = -0.036$  days. In the absence of any photometric data during the elapsed 4724 orbital cycles, we have not been able to decide if the original period was incorrect or was variable, or there was a radial-velocity shift caused by a third body in the system with a possible miscount in the number of orbital cycles.

V335 Peg is one of the brightest short-period binaries in the sky (Rucinski 2002b),  $V_{max} = 7.24$ , and is relatively nearby with the parallax  $16.26 \pm 0.86$  mas, resulting in  $M_V = 3.30 \pm 0.12$ . The color index  $(B - V) = 0.439$  corresponds to the spectral type of F5, which is the same as found in our spectra, F5V. This does not agree well with the RD97 calibration,  $M_V(cal) = 1.85$ . The reason for this discrepancy is not clear. We note that V335 Peg is a source of X-ray radiation and is listed in ROSAT Bright Survey (Schwope et al. 2000). The proper motions of V335 Peg are large in both coordinates (Høg et al. 2000), which – when coupled with the moderate distance of 62 pc – results in a combined spatial velocity of  $V = 58$  km s<sup>-1</sup>.

### 3. SUMMARY

This paper presents spectral classifications, radial velocity data and circular orbital solutions for the eighth group of ten close binary systems observed at the David Dunlap Observatory. All systems are double-lined (SB2) contact binaries. Half of the systems (V445 Cep, V2082 Cyg, V918 Her, V1363 Ori, V335 Peg) were discovered photometrically by the *Hipparcos* mission and two are well known, frequently observed contact systems (AB And, V502 Oph) which had been previously observed spectroscopically, but for which our broadening function method permitted improvement of the orbital elements. We spectroscopically detected very weak companions of V2082 Cyg, KP Peg and especially V335 Peg. We note that V445 Cep, V2082 Cyg, V918 Her, KP Peg and V335 Peg are bright binaries with the observed  $V_{max} < 7.5$ . They were previously considered in the rigorously selected, magnitude-limited sample of Rucinski (2002b).

This study has been done while W. Pych held the NATO Post-Doctoral Fellowship administered by the Natural Sciences and Engineering Council of Canada (NSERC); he also acknowledges the support from the Polish Grant KBN 2 P03D 029 23. The NSERC supported research of S. M. Rucinski and of R. M. Blake, through a research grant to T. Bolton. W. Ogloza, G. Stachowski and K. Gazeas acknowledge the travel and subsistence support from the NATO collaborative linkage grant PST.CLG.978810 as well as the Polish KBN grant 2-P03D-006-22.

The research has made use of the SIMBAD database, operated at the CDS, Strasbourg, France and accessible through the Canadian Astronomy Data Centre, which is operated by the Herzberg Institute of Astrophysics, National Research Council of Canada.

## REFERENCES

- Abt, H. A. 1985, *ApJS*, 59, 95
- Agerer, F., & Dahm, M. 1995, *IBVS*, 4266, 1
- Aitken, R.G. 1932, *New General Catalogue of Double Stars within 120° of the North Pole* (Carnegie Inst. of Washington Pub., No. 417)(ADS).
- Bell, S. A., Hilditch, R. W., & King, D. J. 1984, *MNRAS*, 208, 123
- Bessell, M. S. 1979, *PASP*, 91, 589
- Binnendijk, L. 1969, *AJ*, 74, 218
- Demircan, O., Derman, E., Akalin, A., Selam, S., & MUYESSEROGLU, Z. 1994, *MNRAS*, 267, 19
- Djurasevic, G., Rovithis-Livaniou, H., & Rovithis, P. 2000, *A&A*, 364, 543
- Grenier, S., Baylac, M.-O., Rolland, L., Burnage, R., Arenou, F., Briot, D., Delmas, F., Duflot, M., Genty, V., Gmez, A. E., Halbwegs, J.-L., Marouard, M., Oblak, E., & Sellier, A. 1999, *A&AS*, 137, 451
- Gomez-Forrellad, J. M., Garcia-Melendo, E., Guarro-Flo, J., Nomen-Torres, J., & Vidal-Sainz, J. 1999, *IBVS*, 4702
- Guthnick, P., & Prager, R. 1927, *Kleinere Veröff. Berlin-Babelsberg*, No. 4, 16
- Hendry, P. D., Mochnacki, S. W. 1998, *ApJ*, 504, 978
- Hoffleit, D. 1979, *BICDS*, 17, 24
- Hoffmeister, C. 1935, *Astron. Nachr.*, 255, 403
- Høg, E., Fabricius, C., Makarov, V. V., Urban, S., Corbin, T., Wycoff, G., Bastian, U., Schwekendiek, P., & Wicenec, A. 2000, *A&A*, 355L, 27
- Hopmann, J. 1948, *Z. Astrophysics*, 24, 263
- Hrivnak, B. J. 1988, *ApJ*, 335, 319
- Hughes, V. A., McLean, B. J. 1984, *ApJ*, 278, 716
- Kholopov, P. N., et al. 1985-1988, *General Catalogue of Variable Stars* (4th ed.; Moscow: Nauka)
- Kreiner, J. M. 2003, private communication
- Landolt, A. U. 1969, *AJ*, 74, 1078
- Lause, F. 1937, *Astron. Nachr.*, 264, 106

- Layden, A. C. 1994, AJ, 108, 1016
- Lu, W., & Rucinski, S. M. 1993, AJ, 106, 361
- Lu, W., & Rucinski, S. M. 1999, AJ, 118, 515 (Paper I)
- Lu, W., Rucinski, S. M., & Ogloza, W. 2001, AJ, 122, 402 (Paper IV)
- Nesterov, V. V., Kuzmin, A. V., Ashimbaeva, N. T., Volchkov, A. A., Rser, S., & Bastian, U. 1995, A&AS, 110, 367
- Oja, T. 1991, A&AS, 89, 415
- Oja, T. 1994, IBVS, 4000, 1
- Oosterhoff, P. Th. 1930, Bull. Astron. Inst. Netherlands, 5, 151
- Oosterhoff, P. Th. 1950, Bull. Astron. Inst. Netherlands, 11, 217
- Pribulla, T., Vanko, M., Parimucha, S., Chochol, D. 2002, IBVS, 5341, 1
- Pych, W., 2003, PASP, submitted (astro-ph/0311290)
- Rucinski, S. M 1995, AJ, 109, 2690
- Rucinski, S. M 2002a, AJ, 124, 1746 (Paper VII)
- Rucinski, S. M. 2002b, PASP, 114, 1124
- Rucinski, S. M., Capobianco, C. C., Lu, W., DeBond, H., Thomson, J. R., Mochnacki, S. W., Blake, R. M., Ogloza, W., Stachowski, G., & Rogoziecki, P. 2003, AJ, 125, 3258 (Paper VIII)
- Rucinski, S. M., & Duerbeck, H.W. 1997, PASP, 109, 1340 (RD97)
- Rucinski, S. M., & Kaluzny, J. 1981, AcA, 31, 409
- Rucinski, S. M., & Lu, W. 1999, AJ, 118, 2451 (Paper II)
- Rucinski, S. M., Lu, W., Capobianco, C. C., Mochnacki, S. W., Blake, R. M., Thomson, J. R., Ogloza, W., & Stachowski, G. 2002, AJ, 124, 1738 (Paper VI)
- Rucinski, S. M., Lu, W., & Mochnacki, S. W. 2000, AJ, 120, 1133 (Paper III)
- Rucinski, S. M., Lu, W., Mochnacki, S. W., Ogloza, W., & Stachowski, G. 2001, AJ, 122, 1974 (Paper V)
- Solano, E., Garrido, R., Fernley, J., & Barnes, T. G. 1997, A&AS, 125, 321
- Smith, H. A. 1990, PASP, 102, 124



- Schwope, A., Hasinger, G., Lehmann, I., Schwarz, R., Brunner, H., Neizvestny, S., Ugryumov, A., Balega, Yu., Trümper, J., & Voges, W. 2000, *Astr. Nachr.*, 321, 1
- Strohmeier, W. 1958, *Kl. Verffent. der Sternwarte Bamberg*, No. 24
- Strohmeier, W. et al., 1965, *Verffent. der Sternwarte Bamberg*, Bd., V, No. 18
- Struve, O., Gratton, L. 1948, *ApJ*, 108, 497
- Struve, O., Horak, H. G., Canavaggia, R., Kourganoff, V., & Colacevich, A. 1950, *ApJ*, 111, 658
- Struve, O., Zebergs, V. 1959, *ApJ*, 130, 789
- Shajn, G. A. 1951, *Bull. Crimean Astrophys. Obs.*, 7, 124
- Walker, R. L. 1987, *BAAS*, 19, 1085
- Walker, R. L. 1988, *IBVS*, 19, 1085



Table 1. DDO observations of the eighth group of ten close binary systems

HJD-2,400,000	Phase	$V_1$	$\Delta V_1$	$V_2$	$\Delta V_2$
<b>AB And</b>					
52494.8051	0.1749	-235.6	-0.7	94.5	6.0
52494.8176	0.2126	-251.7	2.3	98.8	-0.4
52494.8284	0.2451	-260.6	-0.2	99.8	-2.9
52495.6065	0.5896	97.0 <sup>a</sup>	0.2	-111.7 <sup>a</sup>	-14.6
52495.6176	0.6231	129.0	-6.2	-122.8	-4.2
52495.6297	0.6597	166.3	-2.5	-135.3	2.1
52495.6406	0.6924	187.2	-3.1	-149.4	0.0
52495.6532	0.7305	200.7	-2.9	-160.5	-3.7
52495.6638	0.7624	202.8	-1.8	-157.0	0.5
52495.6759	0.7989	194.8	0.3	-148.1	3.7
52495.6866	0.8311	179.1	3.4	-147.0	-5.7
52495.7003	0.8723	146.5	6.5	-127.4	-6.2
52496.6651	0.7793	206.5	5.1	-152.0	3.6
52496.6758	0.8116	190.1	2.0	-152.7	-4.5
52496.6884	0.8495	167.0	5.7	-136.1	-2.9
52496.6995	0.8828	140.2	11.4	-122.0	-6.9
52496.7120	0.9206	103.3 <sup>a</sup>	19.4	-110.2 <sup>a</sup>	-20.3
52496.7232	0.9544	...	...	...	...
52496.7353	0.9909	...	...	...	...
52496.7625	0.0728	...	...	...	...
52496.7740	0.1073	-180.6 <sup>a</sup>	-7.6	69.6 <sup>a</sup>	15.7
52496.7867	0.1458	-217.7	-5.4	80.7	4.8
52496.7977	0.1788	-240.2	-2.7	87.9	-2.1
52496.8101	0.2161	-251.9	3.2	102.5	2.6

Table 1—Continued

HJD-2,400,000	Phase	V <sub>1</sub>	ΔV <sub>1</sub>	V <sub>2</sub>	ΔV <sub>2</sub>
52496.8209	0.2487	-258.0	2.4	98.4	-4.4
52496.8334	0.2864	-249.8	4.5	79.8	-19.6
52496.8444	0.3196	-239.0	-0.5	87.0	-3.5
52497.8064	0.2179	-253.8	1.9	96.3	-3.9
52497.8170	0.2501	-258.4	2.0	94.0	-8.8
52497.8289	0.2859	-254.5	-0.0	91.6	-7.9
52497.8397	0.3185	-231.9	7.3	91.8	0.9
52497.8521	0.3557	-204.2	6.7	73.9	-1.2
52497.8633	0.3896	-172.6	3.8	63.6	7.8
52497.8755	0.4263	-134.4 <sup>a</sup>	-2.8	55.5 <sup>a</sup>	24.8
52511.8101	0.4117	-144.8 <sup>a</sup>	5.3	68.0 <sup>a</sup>	26.9
52511.8208	0.4439	...	...	...	...
52511.8330	0.4805	...	...	...	...
52511.8437	0.5129	...	...	...	...
52511.8555	0.5483	...	...	...	...
52511.8663	0.5810	94.8 <sup>a</sup>	8.9	-106.8 <sup>a</sup>	-15.8
52511.8782	0.6169	136.5	8.0	-118.3	-3.4
52511.8890	0.6493	160.7	0.4	-133.6	-1.0
<b>V402 Aur</b>					
52278.6137	0.7156	243.3	-1.7	-1.2	-1.1
52278.6288	0.7407	231.5	-17.9	2.8	3.8
52382.5612	0.9592	...	...	...	...
52518.8562	0.8035	232.8	-5.3	2.2	0.9
52518.8668	0.8212	242.1	12.8	5.7	2.7
52518.8785	0.8405	216.9	-0.0	8.3	2.9

Table 1—Continued

HJD-2,400,000	Phase	$V_1$	$\Delta V_1$	$V_2$	$\Delta V_2$
52518.8891	0.8581	207.0	3.6	10.6	2.4
52518.9008	0.8775	213.2 <sup>a</sup>	27.0	17.5	5.8
52523.7542	0.9197	174.0 <sup>a</sup>	32.2	27.6 <sup>a</sup>	7.0
52523.7652	0.9379	...	...	...	...
52523.7771	0.9576	...	...	...	...
52523.7877	0.9752	...	...	...	...
52523.7997	0.9951	...	...	...	...
52523.8106	0.0131	...	...	...	...
52523.8334	0.0509	...	...	...	...
52529.8878	0.0831	-68.6 <sup>a</sup>	-5.2	63.6 <sup>a</sup>	1.9
52529.8984	0.1007	-85.1	-2.4	67.8	2.2
52602.8057	0.9101	189.3 <sup>a</sup>	36.6	28.6	10.2
52602.8599	0.9997	...	...	...	...
52606.5557	0.1238	-110.9	-5.0	71.3	1.0
52606.5724	0.1515	-138.0	-8.6	76.2	1.2
52606.5908	0.1820	-158.7	-9.3	76.1	-2.9
52606.6072	0.2092	-184.4	-23.1	82.0	0.6
52606.6236	0.2363	-176.7	-9.3	82.0	-0.6
52608.6033	0.5168	...	...	...	...
52608.6884	0.6577	195.7 <sup>a</sup>	-20.0	5.2	-0.6
52608.7052	0.6856	223.9	-9.0	3.8	1.5
52608.7215	0.7126	229.9	-14.1	-1.3	-1.3
52608.7386	0.7410	237.1	-12.3	3.2	4.3
52608.7631	0.7816	236.3	-9.3	4.1	4.4
52608.7800	0.8096	216.4	-18.9	3.4	1.6

Table 1—Continued

HJD-2,400,000	Phase	$V_1$	$\Delta V_1$	$V_2$	$\Delta V_2$
52608.7963	0.8366	216.9	-2.7	7.3	2.4
52608.8125	0.8635	...	...	...	...
52608.8291	0.8910	187.0 <sup>a</sup>	14.0	19.0	4.7
52608.8454	0.9179	185.8 <sup>a</sup>	42.0	28.9 <sup>a</sup>	8.7
52611.8229	0.8518	206.6	-1.9	9.0	1.9
52611.8861	0.9564	...	...	...	...
52611.9084	0.9934	...	...	...	...
52611.9279	0.0257	...	...	...	...
52611.9482	0.0593	...	...	...	...
52612.5317	0.0262	...	...	...	...
52612.5482	0.0535	...	...	...	...
52612.5656	0.0824	...	...	...	...
52612.5833	0.1118	-114.0	-19.8	67.9	-0.0
52612.6001	0.1396	-114.3	5.6	71.3	-1.8
52612.6187	0.1705	-143.0	-0.4	83.7	6.1
52612.6372	0.2010	-158.6	-0.3	84.9	4.1
52612.6541	0.2291	-157.5	8.9	92.7	10.3
52612.6712	0.2574	-160.8	7.1	92.0	9.2
52612.6873	0.2841	-165.0	-1.6	81.0	-0.8
52612.7033	0.3105	-159.4	-6.1	82.8	3.0
52612.7195	0.3374	-139.8	-2.4	81.8	5.2
52612.7360	0.3648	-103.8 <sup>a</sup>	12.3	77.4	5.1
52612.7518	0.3910	-103.4 <sup>a</sup>	-12.0	74.0	6.6
52612.7679	0.4176	...	...	...	...
52612.7837	0.4439	...	...	...	...

Table 1—Continued

HJD-2,400,000	Phase	V <sub>1</sub>	ΔV <sub>1</sub>	V <sub>2</sub>	ΔV <sub>2</sub>
52614.6100	0.4700	...	...	...	...
52614.6256	0.4959	...	...	...	...
52618.8380	0.4759	...	...	...	...
52618.8541	0.5026	...	...	...	...
52618.8701	0.5292	...	...	...	...
52618.9020	0.5821	140.5 <sup>a</sup>	-3.3	18.3 <sup>a</sup>	-1.9
52618.9183	0.6089	183.9 <sup>a</sup>	10.9	18.5	4.2
52618.9183	0.6089	201.4 <sup>a</sup>	28.4	18.9 <sup>a</sup>	4.6
52618.9357	0.6379	189.5 <sup>a</sup>	-10.6	10.3	1.5
<b>V445 Cep</b>					
52382.5883	0.9191	...	...	...	...
52382.5990	0.9429	...	...	...	...
52382.6112	0.9702	...	...	...	...
52382.6222	0.9947	...	...	...	...
52382.6342	0.0215	...	...	...	...
52382.6584	0.0754	...	...	...	...
52382.6700	0.1011	...	...	...	...
52382.6817	0.1273	27.2 <sup>a</sup>	1.1	...	...
52382.6925	0.1513	25.7 <sup>a</sup>	1.6	...	...
52382.7045	0.1779	18.2	-4.2	162.6 <sup>a</sup>	12.1
52382.7151	0.2017	17.9	-3.4	162.6 <sup>a</sup>	5.5
52387.7035	0.3172	17.0	-5.1	163.6 <sup>a</sup>	11.5
52387.7144	0.3416	20.3	-3.3	163.5 <sup>a</sup>	20.4
52387.7266	0.3688	...	...	...	...
52387.7378	0.3937	...	...	...	...

Table 1—Continued

HJD-2,400,000	Phase	$V_1$	$\Delta V_1$	$V_2$	$\Delta V_2$
52387.7498	0.4203	...	...	...	...
52387.7607	0.4446	...	...	...	...
52387.7726	0.4712	...	...	...	...
52387.7835	0.4956	...	...	...	...
52387.7956	0.5225	...	...	...	...
52387.8066	0.5469	...	...	...	...
52387.8186	0.5738	...	...	...	...
52387.8296	0.5982	44.0 <sup>a</sup>	-8.4	...	...
52387.8415	0.6248	50.1	-5.0	-47.4 <sup>a</sup>	-1.9
52388.7572	0.6651	52.6	-5.6	-67.2 <sup>a</sup>	-2.8
52388.7683	0.6898	54.8	-4.8	-74.6	-1.8
52388.7802	0.7165	58.5	-2.1	-79.4	-0.7
52388.7912	0.7410	59.4	-1.6	-79.5	1.7
52388.8032	0.7676	59.5	-1.4	-75.2	5.5
52388.8142	0.7922	60.1	-0.2	-66.9	10.3
52388.8261	0.8186	58.5	-0.7	-70.1	0.1
52388.8371	0.8432	56.4	-1.2	-63.7	-2.7
52416.7670	0.0788	...	...	...	...
52416.7779	0.1032	...	...	...	...
52416.7901	0.1304	28.7 <sup>a</sup>	2.8	...	...
52416.8010	0.1547	25.1 <sup>a</sup>	1.3	...	...
52416.8129	0.1813	22.8	0.5	168.8 <sup>a</sup>	17.3
52416.8239	0.2057	20.8	-0.4	168.9 <sup>a</sup>	10.8
52416.8357	0.2321	19.5	-1.0	178.8 <sup>a</sup>	16.8
52416.8464	0.2559	20.1	-0.2	178.9 <sup>a</sup>	16.2



Table 1—Continued

HJD-2,400,000	Phase	$V_1$	$\Delta V_1$	$V_2$	$\Delta V_2$
52416.8592	0.2843	22.3	1.5	184.3 <sup>a</sup>	24.4
52535.7601	0.2293	12.5	-8.1	173.8 <sup>a</sup>	12.1
52535.7711	0.2538	9.8	-10.6	183.8 <sup>a</sup>	21.0
52535.7833	0.2810	11.9	-8.9	183.9 <sup>a</sup>	23.4
52535.7943	0.3054	14.7	-6.9	189.2 <sup>a</sup>	33.7
52535.8213	0.3657	17.5 <sup>a</sup>	-8.0	...	...
52535.8324	0.3904	...	...	...	...
52535.8447	0.4178	...	...	...	...
52535.8558	0.4425	...	...	...	...
52535.8693	0.4725	...	...	...	...
52535.8800	0.4963	...	...	...	...
52535.8920	0.5231	...	...	...	...
52535.9027	0.5470	...	...	...	...
52535.9149	0.5743	...	...	...	...
52551.5890	0.5005	...	...	...	...
52551.6001	0.5253	...	...	...	...
52551.6123	0.5524	...	...	...	...
52551.6360	0.6053	42.4 <sup>a</sup>	-10.8	...	...
52557.5199	0.7162	58.0	-2.6	-73.9	4.7
52557.5281	0.7346	59.0	-1.9	-72.6	8.2
52557.5376	0.7556	58.1	-2.9	-77.8	3.6
52557.5453	0.7727	59.7	-1.1	-72.3	7.9
52557.5544	0.7932	58.9	-1.4	-59.8	17.2
52557.5618	0.8097	59.4	-0.2	-64.9	8.1
52557.5719	0.8320	54.9	-3.4	-70.5	-5.0

Table 1—Continued

HJD-2,400,000	Phase	V <sub>1</sub>	ΔV <sub>1</sub>	V <sub>2</sub>	ΔV <sub>2</sub>
52557.5792	0.8483	53.3	-4.0	-56.4	2.5
52557.5883	0.8686	49.5	-6.1	-56.0 <sup>a</sup>	-7.0
52557.5956	0.8850	46.4	-7.7	-55.7 <sup>a</sup>	-15.7
52557.6053	0.9065	...	...	...	...
52557.6126	0.9227	...	...	...	...
52557.6227	0.9453	...	...	...	...
52557.6302	0.9621	...	...	...	...
52557.6390	0.9817	...	...	...	...
52557.6464	0.9982	...	...	...	...
52557.6554	0.0182	...	...	...	...
52557.6627	0.0345	...	...	...	...
52557.6714	0.0538	...	...	...	...
<b>V2082 Cyg</b>					
52433.7603	0.6945	-0.1	2.8	-166.9	-1.8
52433.7674	0.7045	0.0	2.3	-166.9	0.9
52433.7755	0.7159	0.4	2.1	-171.9	-1.6
52433.7840	0.7277	1.0	2.3	-166.9	5.2
52433.7921	0.7391	1.3	2.3	-171.9	1.3
52433.7997	0.7497	0.3	1.2	-171.9	1.6
52433.8079	0.7612	0.3	1.3	-171.9	1.2
52433.8153	0.7716	0.7	1.9	-171.9	0.3
52433.8229	0.7822	0.9	2.6	-168.9	1.8
52433.8315	0.7942	-0.3	1.9	-166.9	1.2
52433.8386	0.8041	-0.3	2.5	-163.9	1.6
52433.8457	0.8141	-1.8	1.8	-166.9	-4.6

Table 1—Continued

HJD-2,400,000	Phase	$V_1$	$\Delta V_1$	$V_2$	$\Delta V_2$
52447.6050	0.0826	...	...	...	...
52447.6285	0.1155	...	...	...	...
52447.6410	0.1330	-55.9	2.8	81.5 <sup>a</sup>	12.2
52486.5810	0.6644	-2.2	3.5	-159.9	-6.1
52486.5925	0.6805	-1.4	2.6	-169.9	-9.5
52486.6057	0.6991	-0.2	2.4	-169.7	-3.3
52486.6171	0.7149	-0.0	1.7	-169.8	0.4
52486.6298	0.7327	0.8	1.9	-174.7	-2.0
52486.6406	0.7478	1.1	2.1	-174.7	-1.2
52486.6527	0.7648	0.5	1.6	-174.7	-1.9
52486.6640	0.7806	0.1	1.7	-169.7	1.3
52486.6763	0.7979	-1.3	1.1	-169.8	-2.5
52486.6873	0.8133	-2.0	1.6	-164.6	-2.0
52486.6994	0.8302	-4.0	1.1	-159.7	-3.6
52486.7104	0.8457	-6.7	0.1	-157.8	-8.7
52486.7368	0.8826	-12.2	-0.4	-149.7 <sup>a</sup>	-21.8
52486.7484	0.8988	...	...	...	...
52486.7606	0.9159	...	...	...	...
52486.7716	0.9313	...	...	...	...
52486.7842	0.9490	...	...	...	...
52486.7950	0.9640	...	...	...	...
52486.8076	0.9818	...	...	...	...
52486.8188	0.9975	...	...	...	...
52486.8310	0.0145	...	...	...	...
52486.8421	0.0301	...	...	...	...

Table 1—Continued

HJD-2,400,000	Phase	$V_1$	$\Delta V_1$	$V_2$	$\Delta V_2$
52487.6059	0.0997	...	...	...	...
52487.6134	0.1102	...	...	...	...
52487.6209	0.1207	-54.2	2.7	69.6 <sup>a</sup>	7.9
52487.6294	0.1326	-55.4	3.3	77.0 <sup>a</sup>	8.0
52487.6367	0.1429	-57.5	2.5	77.3 <sup>a</sup>	2.4
52487.6441	0.1532	-59.2	2.1	77.4 <sup>a</sup>	-2.9
52487.6526	0.1651	-60.6	2.1	85.0	-0.9
52487.6600	0.1754	-61.7	2.0	85.1	-5.1
52487.6675	0.1859	-63.0	1.6	85.2	-8.9
52487.6760	0.1979	-62.9	2.6	90.0	-7.9
52487.6834	0.2082	-63.0	3.1	90.0 <sup>a</sup>	-10.5
52491.8017	0.9754	...	...	...	...
52491.8105	0.9878	...	...	...	...
52491.8202	0.0013	...	...	...	...
52491.8290	0.0137	...	...	...	...
52491.8386	0.0272	...	...	...	...
52491.8475	0.0396	...	...	...	...
52491.8578	0.0541	...	...	...	...
52491.8665	0.0662	...	...	...	...
52491.8763	0.0799	...	...	...	...
52491.8850	0.0922	...	...	...	...
52492.7361	0.2840	-62.3	4.2	90.5	-11.6
52492.7453	0.2969	-62.6	3.3	85.5	-13.8
52492.7642	0.3234	-59.5	4.3	83.5	-7.2
52492.7730	0.3356	-58.2	4.4	83.5	-2.1

Table 1—Continued

HJD-2,400,000	Phase	$V_1$	$\Delta V_1$	$V_2$	$\Delta V_2$
52492.7830	0.3497	-56.3	4.7	73.7	-5.1
52492.7918	0.3620	-56.1	3.3	68.7	-3.5
52492.8029	0.3776	-50.6	6.6	68.3 <sup>a</sup>	5.4
52492.8118	0.3900	-50.2	5.0	63.0 <sup>a</sup>	8.3
52492.8217	0.4039	-47.0	6.0	52.5 <sup>a</sup>	7.5
52492.8308	0.4167	...	...	...	...
52492.8440	0.4351	...	...	...	...
52492.8627	0.4613	...	...	...	...
52492.8715	0.4736	...	...	...	...
52495.7229	0.4668	...	...	...	...
52495.7303	0.4771	...	...	...	...
52495.7388	0.4889	...	...	...	...
52495.7461	0.4992	...	...	...	...
52495.7541	0.5104	...	...	...	...
52495.7611	0.5202	...	...	...	...
52495.7696	0.5321	...	...	...	...
52495.7769	0.5424	...	...	...	...
52495.7865	0.5558	...	...	...	...
52495.7937	0.5659	...	...	...	...
52495.8020	0.5775	...	...	...	...
52495.8093	0.5876	-13.2 <sup>a</sup>	3.6	...	...
52495.8192	0.6015	-10.9 <sup>a</sup>	3.5	...	...
52495.8268	0.6121	-9.4 <sup>a</sup>	3.3	...	...
52495.8350	0.6237	-7.8	3.1	-142.2 <sup>a</sup>	-10.3
52495.8421	0.6336	-6.6	2.8	-147.2 <sup>a</sup>	-9.3

Table 1—Continued

HJD-2,400,000	Phase	$V_1$	$\Delta V_1$	$V_2$	$\Delta V_2$
52498.8021	0.7789	-0.0	1.5	-173.0	-1.8
52498.8119	0.7925	0.2	2.3	-176.0	-7.4
52498.8226	0.8076	-0.8	2.3	-168.0	-3.5
52498.8435	0.8368	-3.6	2.2	-153.0	0.2
52498.8614	0.8618	-9.7	-0.9	-143.0 <sup>a</sup>	-2.6
52498.8709	0.8752	-12.6	-1.9	-158.0 <sup>a</sup>	-25.5
52498.8795	0.8872	-16.3	-3.8	-143.0 <sup>a</sup>	-18.1
<b>BX Dra</b>					
52080.6344	0.4384	-38.9 <sup>a</sup>	17.4	...	...
52081.6540	0.1993	-98.8	3.3	183.1 <sup>a</sup>	-53.3
52081.6694	0.2259	-106.4	-1.2	256.5	9.4
52081.6848	0.2524	-99.6	6.6	256.2	6.0
52081.7018	0.2818	-99.4	5.2	256.2	11.4
52081.7174	0.3088	-101.9	-1.2	205.8	-25.9
52081.7332	0.3360	-100.1	-5.4	219.5	8.5
52081.7491	0.3634	-81.2	5.4	206.6	23.6
52081.7643	0.3898	-75.5	1.7	144.9	-5.4
52081.7800	0.4168	-51.2	14.9	179.0 <sup>a</sup>	67.2
52081.7956	0.4438	-31.3 <sup>a</sup>	22.5	...	...
52081.8108	0.4701	-32.1 <sup>a</sup>	9.0	...	...
52389.5501	0.9466	...	...	...	...
52389.5655	0.9732	-8.7 <sup>a</sup>	4.0	...	...
52389.5810	1.0000	-43.1 <sup>a</sup>	-17.0	...	...
52389.5967	0.0272	-55.6	-15.9	67.3 <sup>a</sup>	46.4
52389.6121	0.0537	-57.7	-5.1	69.2 <sup>a</sup>	3.8

Table 1—Continued

HJD-2,400,000	Phase	$V_1$	$\Delta V_1$	$V_2$	$\Delta V_2$
52389.6276	0.0805	-79.6	-14.7	89.5 <sup>a</sup>	-18.3
52389.6429	0.1070	...	...	...	...
52389.6589	0.1345	...	...	...	...
52389.6742	0.1610	-99.3	-5.4	188.3	-19.9
52389.6894	0.1872	-77.0 <sup>a</sup>	23.0	185.1 <sup>a</sup>	-43.9
52395.6908	0.5518	-11.1 <sup>a</sup>	-10.6	-109.6 <sup>a</sup>	4.9
52395.7062	0.5785	1.6 <sup>a</sup>	-10.2	-105.1 <sup>a</sup>	51.9
52395.7220	0.6057	31.3	8.1	-188.4	8.0
52395.7373	0.6322	38.3	5.4	-259.4	-29.3
52395.7529	0.6592	31.4	-9.8	-263.4	-4.7
52395.7685	0.6861	35.9	-11.6	-339.2 <sup>a</sup>	-58.7
52395.7841	0.7130	55.4	3.7	-264.3	30.8
52395.7995	0.7395	49.2	-4.5	-286.4	15.5
52395.8148	0.7659	63.7	10.2	-294.5	6.6
52395.8301	0.7925	62.3	11.2	-306.9	-14.2
52395.8454	0.8188	46.1	-0.4	-267.1 <sup>a</sup>	10.0
52395.8607	0.8452	46.5	6.5	-251.1	3.4
52395.8763	0.8722	31.9	0.5	-237.2	-12.3
52395.8915	0.8986	27.2	5.7	-205.9	-15.3
52416.5740	0.6179	21.8	-6.1	-259.9	-47.3
52416.5903	0.6460	37.9	0.5	-288.1	-42.6
52416.6069	0.6747	42.4	-2.7	-276.8	-4.6
52416.6211	0.6992	38.2	-11.7	-288.3	0.2
52416.6370	0.7267	50.9	-2.2	-283.2	16.4
52416.6531	0.7545	56.6	2.8	-277.2	25.2

Table 1—Continued

HJD-2,400,000	Phase	V <sub>1</sub>	ΔV <sub>1</sub>	V <sub>2</sub>	ΔV <sub>2</sub>
52416.6689	0.7817	48.5	-3.8	-274.2	22.9
52416.6845	0.8087	48.1	-0.4	-277.9	6.0
52416.7021	0.8392	41.2	-0.5	-266.1	-5.8
52416.7178	0.8662	40.6	7.1	-227.6	4.5
52416.7339	0.8940	43.0	19.7	-198.1	-1.2
<b>V918 Her</b>					
52328.8921	0.1742	-205.9	-3.0	22.7	0.5
52328.9074	0.2009	-210.9	4.8	27.1	1.5
52328.9228	0.2277	-211.3	11.9	27.6	-0.1
52328.9385	0.2549	-220.9	4.1	30.0	1.8
52328.9524	0.2791	-205.9	15.9	28.2	0.9
52328.9640	0.2992	-205.9	9.7	28.3	2.7
52346.7880	0.3078	-207.3	4.8	32.7	8.0
52374.7396	0.9353	...	...	...	...
52374.7522	0.9573	...	...	...	...
52374.7656	0.9806	...	...	...	...
52374.7760	0.9988	...	...	...	...
52374.7866	0.0171	...	...	...	...
52374.8027	0.0451	...	...	...	...
52374.8375	0.1057	-147.0 <sup>a</sup>	1.6	3.3 <sup>a</sup>	-4.2
52374.8482	0.1244	-155.9 <sup>a</sup>	10.3	10.4 <sup>a</sup>	-1.8
52374.8598	0.1444	-176.6	6.2	19.1	2.3
52374.8699	0.1621	-197.2	-1.8	21.0	0.8
52374.8821	0.1833	-212.3	-4.4	22.3	-1.2
52374.9013	0.2166	-217.5	3.3	31.1	4.1



Table 1—Continued

HJD-2,400,000	Phase	$V_1$	$\Delta V_1$	$V_2$	$\Delta V_2$
52374.9120	0.2353	-207.0	17.3	31.1	3.1
52391.6294	0.3187	-218.0	-11.2	25.9	2.6
52391.6400	0.3371	-192.6	3.3	23.4	3.0
52391.6520	0.3579	-182.2	-1.2	19.6	3.4
52391.6630	0.3772	-172.2	-7.4	13.9	2.0
52391.6750	0.3980	-143.1	1.9	9.3	2.7
52391.6856	0.4164	-112.1	13.6	-1.2	-2.5
52391.6975	0.4371	-102.1	0.3	-14.9	-10.0
52391.7084	0.4561	...	...	...	...
52391.7204	0.4769	...	...	...	...
52391.7314	0.4960	...	...	...	...
52391.7432	0.5167	...	...	...	...
52391.7543	0.5360	...	...	...	...
52391.7662	0.5566	...	...	...	...
52391.7772	0.5758	88.9 <sup>a</sup>	23.2	-41.9	8.5
52391.7892	0.5966	90.7	2.7	-52.0	4.5
52391.7998	0.6151	107.0	0.8	-59.2	2.3
52391.8125	0.6371	143.0	17.4	-63.7	2.9
52391.8230	0.6554	157.9	18.4	-67.6	2.8
52391.8345	0.6755	158.3	6.1	-72.0	1.9
52391.8455	0.6946	161.6	-0.1	-74.8	1.7
52391.8575	0.7154	165.3	-3.6	-77.1	1.2
52391.8684	0.7344	164.9	-7.8	-78.6	0.7
52391.8801	0.7548	165.0	-8.6	-79.1	0.5
52391.8908	0.7733	169.6	-1.9	-76.9	2.1

Table 1—Continued

HJD-2,400,000	Phase	$V_1$	$\Delta V_1$	$V_2$	$\Delta V_2$
52391.9016	0.7922	165.7	-1.0	-76.7	1.1
52404.7294	0.1088	-157.1 <sup>a</sup>	-5.5	-2.2 <sup>a</sup>	-10.6
52404.7455	0.1368	-186.5	-9.7	11.3	-3.8
52404.7613	0.1643	-207.4	-10.6	16.9	-3.6
52404.7766	0.1908	-216.7	-5.3	21.6	-2.9
52404.7919	0.2176	-227.6	-6.6	26.6	-0.5
52404.8077	0.2449	-217.3	7.7	26.9	-1.3
52404.8233	0.2722	-206.8	16.3	29.2	1.5
52404.8386	0.2987	-222.5	-6.7	25.9	0.2
52422.6113	0.2180	-234.7	-13.6	26.3	-0.8
52422.6225	0.2375	-224.5	-0.1	27.7	-0.3
52422.6344	0.2582	-224.1	0.7	31.0	2.9
52422.6454	0.2773	-218.5	3.7	27.6	0.2
52422.6585	0.3001	-230.1	-14.8	26.6	1.0
52422.6693	0.3189	-230.2	-23.5	25.2	2.0
52422.6962	0.3657	-194.6	-19.9	18.2	3.6
52422.7146	0.3978	-163.7	-18.5	2.0	-4.6
52422.7239	0.4138	-133.6	-5.2	-2.5	-4.6
52779.8033	0.6268	129.2 <sup>a</sup>	12.4	-57.7	6.6
52779.8128	0.6433	...	...	...	...
52781.5844	0.7255	159.0	-12.3	-82.4	-3.4
52781.6023	0.7566	159.5	-14.0	-78.7	1.0
52781.6202	0.7877	152.0	-16.1	-82.8	-4.6
52781.6381	0.8189	146.3	-8.9	-77.8	-3.1
52781.6565	0.8509	145.4	10.5	-68.9	0.2

Table 1—Continued

HJD-2,400,000	Phase	$V_1$	$\Delta V_1$	$V_2$	$\Delta V_2$
52781.6779	0.8881	119.2 <sup>a</sup>	16.0	-59.7	0.9
52781.6980	0.9231	...	...	-46.2	4.6
52781.7156	0.9537	...	...	...	...
52781.7302	0.9791	...	...	...	...
52781.7441	0.0032	...	...	...	...
52781.7568	0.0253	...	...	...	...
<b>V502 Oph</b>					
52410.7676	0.4051	-177.2	3.9	18.2	14.4
52410.7831	0.4393	-126.4 <sup>a</sup>	8.0	11.6 <sup>a</sup>	23.4
52410.7974	0.4708	...	...	...	...
52445.5895	0.2086	-285.0	-4.0	33.5	-3.9
52445.6009	0.2337	-287.8	0.1	35.6	-4.1
52445.6141	0.2628	-284.6	3.8	37.3	-2.6
52445.6250	0.2867	-279.9	2.8	34.9	-3.1
52445.6372	0.3137	-267.8	2.0	33.1	-0.5
52445.6486	0.3390	-256.6	-4.9	27.2	-0.4
52445.6608	0.3658	-227.7	-0.9	24.5	5.3
52445.6715	0.3894	-201.9	-1.4	19.6	9.2
52445.6826	0.4139	-162.8	6.9	12.6	12.6
52445.6963	0.4441	-138.8 <sup>a</sup>	-11.3	-6.4 <sup>a</sup>	7.7
52445.7078	0.4695	...	...	...	...
52445.7202	0.4969	...	...	...	...
52445.7313	0.5213	...	...	...	...
52445.7441	0.5494	24.6 <sup>a</sup>	-8.2	...	...
52445.7668	0.5996	103.5	1.6	-97.2	-6.2

Table 1—Continued

HJD-2,400,000	Phase	$V_1$	$\Delta V_1$	$V_2$	$\Delta V_2$
52445.7668	0.5996	103.7	1.8	-97.1	-6.1
52445.7779	0.6240	126.3	-4.5	-104.7	-4.0
52445.8152	0.7063	193.4	-1.5	-117.2	4.9
52445.8152	0.7063	193.4	-1.5	-117.4	4.7
52445.8258	0.7297	202.5	0.4	-116.7	7.9
52446.5953	0.4270	-149.0 <sup>a</sup>	2.8	5.6 <sup>a</sup>	11.5
52446.6063	0.4512	-132.9 <sup>a</sup>	-15.9	-20.1 <sup>a</sup>	-2.5
52446.6184	0.4778	...	...	...	...
52446.6290	0.5012	...	...	...	...
52446.6410	0.5276	...	...	...	...
52446.6521	0.5522	27.2 <sup>a</sup>	-9.8	...	...
52446.6641	0.5787	80.4	6.0	-96.0	-14.2
52446.6758	0.6045	109.8	1.7	-106.0	-12.9
52446.6878	0.6308	137.6	-0.5	-109.1	-5.9
52446.6988	0.6551	159.8	-1.8	-116.5	-5.5
52446.7106	0.6813	182.4	0.9	-115.5	2.2
52446.7216	0.7054	192.7	-1.8	-123.7	-1.6
52446.7337	0.7321	187.8	-14.7	-125.1	-0.4
52446.7447	0.7563	205.0	1.0	-123.2	2.0
52446.7568	0.7832	198.0	-0.8	-121.9	1.6
52446.7677	0.8071	185.7	-2.7	-125.2	-5.2
52446.7790	0.8322	...	...	...	...
52492.5910	0.8752	147.3	15.7	-91.5	9.4
52492.6065	0.9095	107.2	16.9	-78.4	8.7
52492.6219	0.9435	...	...	...	...

Table 1—Continued

HJD-2,400,000	Phase	V <sub>1</sub>	ΔV <sub>1</sub>	V <sub>2</sub>	ΔV <sub>2</sub>
52492.6375	0.9778	...	...	...	...
52492.6528	0.0117	...	...	...	...
52492.6687	0.0466	...	...	...	...
52492.6860	0.0848	...	...	...	...
52493.5837	0.0648	...	...	...	...
52493.6000	0.1007	-198.3	-9.9	8.6	2.3
52493.6175	0.1394	-244.7	-12.6	19.0	-2.0
52493.6332	0.1739	-266.7	-5.1	29.6	-1.2
52493.6488	0.2083	-279.4	1.5	30.6	-6.7
52493.6637	0.2414	-284.9	4.0	34.7	-5.3
52493.6793	0.2758	-281.5	4.5	37.3	-1.7
52494.5820	0.2668	-284.0	3.9	35.5	-4.2
52494.5975	0.3009	-272.7	4.1	37.0	1.1
52494.6136	0.3364	-256.0	-2.2	25.3	-3.0
<b>V1363 Ori</b>					
52561.9274	0.2174	-3.8	2.2	276.8	24.2
52561.9454	0.2590	3.4	10.3	297.8	41.0
52562.9110	0.4946	...	...	...	...
52562.9281	0.5342	...	...	...	...
52562.9450	0.5733	...	...	...	...
52567.8756	0.9888	...	...	...	...
52571.8052	0.0868	-31.5 <sup>a</sup>	-46.2	121.0 <sup>a</sup>	-30.6
52571.8224	0.1266	-16.9 <sup>a</sup>	-22.7	173.2 <sup>a</sup>	-21.3
52571.8387	0.1643	-21.2 <sup>a</sup>	-20.6	198.4 <sup>a</sup>	-27.8
52571.8551	0.2023	-4.6	0.3	250.7	3.3

Table 1—Continued

HJD-2,400,000	Phase	$V_1$	$\Delta V_1$	$V_2$	$\Delta V_2$
52571.8716	0.2405	-6.7	0.2	270.0	13.2
52571.8886	0.2799	-8.6	-2.4	248.0	-5.3
52571.9050	0.3180	0.9	3.8	257.7	20.2
52571.9215	0.3562	-9.4	-12.0	181.5	-28.7
52575.9216	0.6174	56.1	-12.0	-122.8 <sup>a</sup>	-13.3
52575.9385	0.6563	47.8	-27.4	-123.6	20.9
52576.9520	0.0028	...	...	...	...
52618.6031	0.4351	-4.4 <sup>a</sup>	-24.5	126.0 <sup>a</sup>	1.2
52618.6193	0.4727	-8.6 <sup>a</sup>	-38.8	91.8 <sup>a</sup>	16.4
52618.6377	0.5152	...	...	...	...
52618.6535	0.5518	...	...	...	...
52618.6700	0.5900	35.8 <sup>a</sup>	-26.1	-34.2 <sup>a</sup>	45.4
52618.6859	0.6268	58.1	-11.9	-148.5	-29.6
52618.7019	0.6639	65.1	-11.2	-154.4	-4.4
52618.7179	0.7010	73.7	-7.0	-231.5 <sup>a</sup>	-60.4
52618.7342	0.7386	78.9	-3.8	-165.5	15.4
52618.7509	0.7773	70.4	-11.7	-179.5	-1.3
52618.7671	0.8148	85.0	5.9	-128.4	35.1
52618.7830	0.8515	80.5	6.6	-123.7	14.6
52618.7988	0.8883	83.5	16.6	-89.6	14.1
52618.8156	0.9272	77.1	19.4	-86.4 <sup>a</sup>	-27.4
52619.6081	0.7620	60.2	-22.4	-165.0	15.8
52619.6247	0.8003	78.6	-1.9	-174.7	-4.2
52619.6429	0.8424	78.6	3.2	-146.9	-1.5
52619.6599	0.8819	91.0	22.8	-93.5	16.9

Table 1—Continued

HJD-2,400,000	Phase	$V_1$	$\Delta V_1$	$V_2$	$\Delta V_2$
52619.6789	0.9258	64.7	6.7	-83.9 <sup>a</sup>	-23.2
52619.6958	0.9650	...	...	...	...
52619.7125	0.0036	...	...	...	...
52619.7306	0.0455	...	...	...	...
52619.7475	0.0847	28.0 <sup>a</sup>	12.9	105.8 <sup>a</sup>	-43.4
52619.7669	0.1297	-20.3 <sup>a</sup>	-25.5	162.0 <sup>a</sup>	-35.4
52619.7885	0.1797	2.6	5.3	234.7	-1.4
52619.8053	0.2185	1.8	8.0	270.4	17.4
52619.8221	0.2573	-12.4	-5.5	237.8 <sup>a</sup>	-19.2
52619.8385	0.2953	-6.0	-0.8	268.9	20.5
52619.8547	0.3328	-4.3	-3.2	211.3	-16.9
52621.5781	0.3230	-21.6	-19.2	240.9	6.4
52621.5943	0.3605	-7.1	-10.5	205.5	-1.0
52621.6109	0.3989	-13.1 <sup>a</sup>	-24.4	156.5 <sup>a</sup>	-11.5
52621.6277	0.4378	-36.0 <sup>a</sup>	-56.8	112.4 <sup>a</sup>	-9.1
<b>KP Peg</b>					
52497.7545	0.1323	-38.1	10.2	179.2 <sup>a</sup>	6.4
52497.7642	0.1456	-44.8	7.4	199.4	14.4
52497.7732	0.1580	-51.2	4.3	179.3 <sup>a</sup>	-15.9
52497.7806	0.1682	-54.1	3.8	189.4 <sup>a</sup>	-13.3
52497.7888	0.1794	-52.0	8.2	...	...
52497.7960	0.1894	-61.4	0.7	189.7 <sup>a</sup>	-26.1
52499.6615	0.7547	81.7	3.3	-221.4 <sup>a</sup>	-0.6
52499.6721	0.7693	83.3	5.5	-191.4 <sup>a</sup>	27.8
52499.6842	0.7859	91.9	15.4	-191.6 <sup>a</sup>	23.6

Table 1—Continued

HJD-2,400,000	Phase	$V_1$	$\Delta V_1$	$V_2$	$\Delta V_2$
52499.6951	0.8009	74.3	-0.4	-221.1	-11.7
52499.7074	0.8179	74.9	3.0	-201.3	-0.7
52499.7184	0.8330	71.8	3.1	-201.3	-10.5
52499.7346	0.8553	69.2	6.2	-171.4 <sup>a</sup>	1.8
52499.7452	0.8698	61.7	3.0	-171.2 <sup>a</sup>	-11.5
52499.7577	0.8870	55.8	2.8	-191.2 <sup>a</sup>	-49.1
52499.7690	0.9025	51.6	4.2	...	...
52499.7816	0.9199	44.0	3.3	...	...
52499.7924	0.9346	41.3	6.7	...	...
52499.8055	0.9528	47.3	20.5	...	...
52499.8177	0.9695	16.0	-3.4	...	...
52499.8304	0.9870	6.9	-4.6	...	...
52499.8412	0.0018	-4.4	-9.1	...	...
52506.7039	0.4390	-19.7	2.1	...	...
52506.7146	0.4537	-8.5	6.8	...	...
52506.7264	0.4699	-3.6	4.5	...	...
52506.7370	0.4845	0.6	2.2	...	...
52506.7489	0.5009	10.1	4.1	...	...
52506.7599	0.5159	12.6	-0.2	...	...
52506.7728	0.5336	23.0	2.2	...	...
52506.7815	0.5456	30.7	4.6	...	...
52506.7896	0.5567	34.1	3.1	...	...
52506.7971	0.5670	36.3	0.9	...	...
52506.8057	0.5790	45.3	5.1	...	...
52506.8132	0.5893	48.6	4.3	...	...



Table 1—Continued

HJD-2,400,000	Phase	$V_1$	$\Delta V_1$	$V_2$	$\Delta V_2$
52506.8253	0.6059	48.4	-2.1	-144.6 <sup>a</sup>	-10.3
52506.8325	0.6157	61.0	7.1	-145.0 <sup>a</sup>	0.0
52506.8410	0.6275	59.0	1.1	...	...
52506.8483	0.6376	58.4	-2.5	...	...
52506.8569	0.6493	68.2	3.9	...	...
52506.8647	0.6601	67.0	-0.1	...	...
52506.8743	0.6733	63.1	-7.0	...	...
52506.8840	0.6866	61.9	-10.7	...	...
52507.6205	0.6994	87.1	12.4	-225.4 <sup>a</sup>	-15.9
52507.6279	0.7095	81.7	5.7	-225.4 <sup>a</sup>	-11.8
52507.6373	0.7225	79.4	2.1	-225.4 <sup>a</sup>	-7.8
52507.6460	0.7345	78.4	0.4	-244.9	-25.1
52507.6557	0.7478	72.2	-6.2	-244.9	-24.0
52507.6632	0.7581	62.8	-15.5	-194.6 <sup>a</sup>	26.0
52508.6157	0.0679	-32.7	-8.1	...	...
52508.6374	0.0977	-42.4	-6.0	...	...
52508.6452	0.1085	-41.7	-1.4	...	...
52508.6558	0.1230	-46.4	-1.1	174.6 <sup>a</sup>	11.0
52508.7143	0.2034	-60.3 <sup>a</sup>	3.9	224.4 <sup>a</sup>	2.1
52511.6430	0.2309	-63.1	3.7	223.1	-7.2
52511.6520	0.2432	-66.2	1.1	223.2	-8.6
52511.6617	0.2566	-72.1	-4.8	223.3	-8.5
52511.6704	0.2685	-74.7	-7.9	193.3	-37.1
52511.6815	0.2838	-68.3	-2.7	223.3	-3.6
52511.6917	0.2978	-60.7	3.4	193.1	-28.7

Table 1—Continued

HJD-2,400,000	Phase	$V_1$	$\Delta V_1$	$V_2$	$\Delta V_2$
52511.7015	0.3113	-58.5	3.5	213.1	-2.2
52511.7102	0.3232	-58.9	0.8	203.0	-5.4
52511.7199	0.3366	-58.4	-1.6	203.0 <sup>a</sup>	3.7
52511.7286	0.3486	-51.1	2.7	202.8	12.9
52511.7385	0.3622	-44.0	5.9	202.5 <sup>a</sup>	24.5
52511.7473	0.3743	-41.5	4.7	193.2 <sup>a</sup>	26.8
52511.7572	0.3879	-30.7	11.0	182.8 <sup>a</sup>	30.6
52511.7659	0.3998	-29.2	8.2	...	...
52511.7762	0.4140	-26.7	5.3	...	...
52511.7855	0.4268	-26.7	0.1	...	...
<b>V335 Peg</b>					
52130.7623	0.8919	13.5	0.9	-120.7 <sup>a</sup>	1.9
52130.7767	0.9098	7.7	-0.8	-120.6 <sup>a</sup>	-13.6
52130.7921	0.9287	2.7	-1.2	...	...
52130.8078	0.9481	-2.2	-1.0	...	...
52130.8233	0.9672	-8.2	-1.9	...	...
52130.8385	0.9860	-12.4	-0.9	...	...
52130.8537	0.0047	-17.6	-0.9	...	...
52130.8694	0.0240	-23.9	-1.7	...	...
52130.8826	0.0403	-27.6	-1.1	...	...
52493.7074	0.5744	5.0	0.3	...	...
52493.7227	0.5933	9.8	0.5	-119.1	-9.4
52493.7366	0.6104	14.0	0.9	-119.2	5.3
52493.7474	0.6237	16.5	0.6	-129.1	5.9
52493.7601	0.6394	20.3	1.4	-129.2	17.3

Table 1—Continued

HJD-2,400,000	Phase	$V_1$	$\Delta V_1$	$V_2$	$\Delta V_2$
52493.7709	0.6527	20.4	-0.7	-149.1	5.9
52493.7829	0.6676	24.4	1.0	-169.2	-5.5
52493.7937	0.6808	25.3	0.3	-169.2	1.0
52493.8063	0.6965	26.9	0.2	-189.1	-12.7
52493.8170	0.7096	27.3	-0.5	-179.2	1.3
52494.6392	0.7237	29.6	1.0	-181.2	2.4
52494.6500	0.7371	30.2	1.2	-191.2	-5.8
52494.6626	0.7526	30.7	1.5	-191.2	-5.3
52494.6735	0.7660	29.9	0.9	-191.2	-6.1
52494.6856	0.7810	29.9	1.6	-181.2	1.5
52494.6966	0.7946	28.0	0.5	-181.2	-1.9
52494.7689	0.8838	14.7	0.4	-121.3	7.9
52494.7814	0.8992	11.2	0.2	-121.3	-4.9
52494.7921	0.9123	7.2	-0.7	-121.3 <sup>a</sup>	-16.6
52498.7436	0.7865	27.2	-0.8	-178.6	2.9
52498.7525	0.7974	26.3	-0.9	-178.6	-0.2
52498.7626	0.8099	25.7	-0.4	-178.6 <sup>a</sup>	-4.6
52498.7711	0.8203	23.5	-1.5	-178.6 <sup>a</sup>	-9.0
52498.7805	0.8320	23.6	0.2	-178.6 <sup>a</sup>	-14.8
52498.7892	0.8426	21.6	-0.2	-178.6 <sup>a</sup>	-20.7
52500.7044	0.2050	-59.1	-0.9	148.6	0.3
52500.7166	0.2201	-60.3	-1.1	148.6	-3.5
52500.7364	0.2445	-59.9	0.1	...	...
52500.7871	0.3070	-57.8	-0.6	138.6	-5.7
52500.7978	0.3202	-56.0	-0.3	...	...

Table 1—Continued

HJD-2,400,000	Phase	$V_1$	$\Delta V_1$	$V_2$	$\Delta V_2$
52500.8096	0.3348	-54.8	-1.0	138.6	7.1
52500.8204	0.3481	-51.8	0.0	138.6	14.8
52500.8329	0.3635	-50.1	-0.9	118.6	5.0
52500.8508	0.3856	-44.3	0.5	118.6	21.7
52500.8624	0.3999	-40.4	1.3	98.7	13.7
52500.8730	0.4129	-39.3	-0.7	88.6	15.2
52500.8846	0.4273	-35.8	-0.7	88.5	28.7
52500.8952	0.4404	-32.2	-0.4	68.7	21.7
52514.7381	0.5151	-12.1	-1.0	...	...
52514.7504	0.5304	-8.5	-1.6	...	...
52514.7623	0.5450	-4.2	-1.2	...	...
52514.7742	0.5597	-0.6	-1.5	...	...
52514.7866	0.5750	3.7	-1.1	...	...
52518.5450	0.2108	-60.0	-1.3	142.2	-7.8
52518.5571	0.2258	-59.2	0.3	142.2	-11.0
52518.5693	0.2408	-59.2	0.7	162.2	7.3
52518.5810	0.2553	-58.1	1.9	192.2 <sup>a</sup>	37.1
52518.5909	0.2675	-60.1	-0.4	182.2	28.1
52518.5994	0.2780	-59.4	-0.0	132.2	-20.4
52518.6080	0.2886	-58.5	0.2	152.2	2.0
52518.6157	0.2980	-57.9	0.1	152.2	4.7
52518.6258	0.3105	-56.3	0.6	152.2	9.2
52518.6327	0.3191	-56.2	-0.3	102.2	-37.2
52518.6410	0.3293	-54.5	0.1	112.1	-22.3
52518.6478	0.3377	-53.9	-0.5	122.2	-7.8

Table 1—Continued

HJD-2,400,000	Phase	$V_1$	$\Delta V_1$	$V_2$	$\Delta V_2$
52518.6547	0.3462	-51.1	1.0	112.1	-12.8
52518.6629	0.3563	-50.0	0.5	102.1	-16.4
52518.6725	0.3682	-47.6	0.7	102.1	-8.1
52518.6784	0.3754	-46.8	0.0	92.1	-12.8
52518.6855	0.3842	-43.5	1.6	112.1	14.1
52518.6914	0.3914	-41.7	1.8	112.2	20.0
52518.6986	0.4003	-40.7	0.8	92.1	7.5
52518.7039	0.4069	-38.6	1.4	92.1	13.4
52518.7093	0.4136	-39.1	-0.7	72.1	-0.6
52518.7158	0.4216	-35.3	1.2	82.0	16.7
52518.7239	0.4315	-32.3	1.7	82.0	26.3
52518.7290	0.4379	-30.9	1.5	62.1	12.6
52518.7360	0.4465	-28.7	1.4	62.2	21.3
52518.7417	0.4535	-27.6	0.7	52.1	18.4
52518.7490	0.4624	-23.3	2.6	...	...
52518.7553	0.4703	-21.1	2.6	...	...
52518.7628	0.4795	-19.1	2.0	...	...
52518.7690	0.4872	-16.6	2.4	...	...
52518.7760	0.4958	-15.7	0.9	...	...
52518.7813	0.5023	-13.6	1.2	...	...
52518.7877	0.5103	-12.3	0.2	...	...
52518.7930	0.5168	-9.2	1.5	...	...
52518.7997	0.5250	-7.9	0.5	...	...
52518.8048	0.5314	-6.8	-0.2	...	...
52518.8116	0.5397	-5.2	-0.8	...	...

Table 1—Continued

HJD-2,400,000	Phase	$V_1$	$\Delta V_1$	$V_2$	$\Delta V_2$
52518.8171	0.5465	-3.0	-0.4	...	...
52518.8227	0.5534	-1.0	-0.3	...	...
52518.8291	0.5613	0.0	-1.3	...	...
52518.8342	0.5676	1.7	-1.3	...	...
52529.6969	0.9665	-7.7	-1.6	...	...
52529.7080	0.9801	-13.1	-3.2	...	...
52529.7190	0.9936	-15.6	-2.0	...	...
52529.7288	0.0058	-19.0	-2.0	...	...
52529.7404	0.0201	-22.9	-1.8	...	...
52529.7510	0.0332	-25.4	-0.7	...	...
52529.7627	0.0476	-30.2	-1.6	...	...
52529.7738	0.0612	-34.0	-1.8	...	...
52529.7860	0.0763	-38.3	-2.3	83.5 <sup>a</sup>	20.3
52529.7966	0.0895	-42.8	-3.7	83.6 <sup>a</sup>	8.1
52529.8102	0.1062	-46.0	-3.0	83.6	-6.5
52529.8209	0.1193	-48.8	-3.0	103.5	2.7
52529.8325	0.1337	-51.7	-3.1	103.5	-8.1
52529.8431	0.1468	-54.3	-3.3	103.6	-17.0
52529.8547	0.1610	-55.8	-2.6	113.5	-15.7
52529.8653	0.1741	-58.1	-3.1	133.5	-2.6
52529.8773	0.1889	-59.9	-3.2	143.5	0.7

<sup>a</sup>The data given 0.5 weight in the orbital solution.

Note. — Velocities are expressed in  $\text{km s}^{-1}$ . The deviations  $\Delta V_i$  are relative to the simple sine-curve fits to the radial velocity data. Observations leading to entirely unseparable broadening- and correlation-function peaks are marked by the “no-data” symbol ( ... ); these observations may be eventually used in more extensive modeling of broadening functions.